

# A SPECTROSCOPIC STUDY OF RHODOPSIN ALPHA-HELIX ORIENTATION

K. J. ROTHSCHILD, R. SANCHES, AND T. L. HSIAO *Department of Physics and  
Department of Physiology, Boston University, Boston, Massachusetts 02215*  
N. A. CLARK, *Department of Physics, University of Colorado, Boulder, Colorado  
80309 U.S.A.*

**ABSTRACT** Polarized Fourier transform infrared spectroscopy and far ultraviolet circular dichroism of oriented multilamellar films of photoreceptor membranes indicate rhodopsin alpha-helices are predominantly oriented perpendicular to the bilayer plane.

The fluid globular protein model has been extremely successful in describing the overall organization of cellular membranes (1). However, detailed information is still unavailable about the structure of integral membrane proteins, the key components of membrane transport, and other important membrane mediated processes. The chief difficulty has been the inability to crystallize integral membrane proteins. One approach to this problem is the utilization of multilamellar arrays formed from lipids or natural membrane components (2, 3). This method has the advantage of allowing the use of a variety of biophysical techniques capable of detecting the orientation of specific protein groups.

We have sought to develop improved methods of incorporating biomembranes into multilamellar arrays without destroying the membranes' functional properties (4-6), and to apply spectroscopic methods able to probe membrane structure. As a test of our approach, we have chosen to investigate photoreceptor membrane and its major protein, rhodopsin (7). While it is known that the absorption of light by the retinylidene chromophore of rhodopsin triggers a series of conformational changes, only limited information has been obtained about these changes or about the structure of rhodopsin. Raman spectroscopy (8), infrared spectroscopy (9, 10), and circular dichroism (11) indicate that rhodopsin contains extensive alpha-helices but little beta-structure. Furthermore, chemical labeling shows rhodopsin spanning the bilayer (12). Since a related protein, bacteriorhodopsin, from the purple membrane of *Halobacterium halobium* (13) has been found to contain seven alpha-helical segments oriented predominantly perpendicular to the membrane plane (14), the question arises whether other membrane proteins such as rhodopsin contain a similar structure. Unfortunately the electron diffraction method which has been applied to purple membrane depends on the existence of a periodic lattice of membrane proteins and is therefore not generally applicable to most membranes. In contrast, the spectroscopic methods described here can be applied to all biological and reconstituted membranes which can be incorporated into a multilamellar array without loss of biological activity.

We have utilized two different spectroscopic techniques, polarized infrared (IR) spectroscopy and far ultraviolet circular dichroism (UVCD), to obtain information about the orientation of alpha-helices in rhodopsin. The recent application of both of these techniques

(15, 16) to oriented arrays of purple membrane demonstrates their ability to detect predominantly perpendicular alpha-helices. By measuring the linear dichroism of the infrared amide I, II, and A absorption bands, it is possible to obtain an upper-limit estimate of the average alpha-helix tilt relative to the membrane plane (15). In the case of far UVCD, the disappearance of the 210-nm pi-pi\* transition band, which is active only when the light is incident perpendicular to the alpha-helix axis, can also indicate the existence of alpha-helices predominantly arranged perpendicular to the membrane plane.

To use polarized infrared or circular dichroism measurements to obtain information about protein group orientation, it is necessary that the membrane fragments be oriented relative to a macroscopic sample plane. We have recently developed a method (isopotential spin-drying) which produces well oriented multilamellar arrays of photoreceptor membranes up to 50  $\mu\text{m}$  thick (6). These samples are suitable for polarized infrared and circular dichroism measurements as well as a number of other biophysical techniques. Furthermore, the rhodopsin in these films appears to remain active and structurally intact (4, 10) as based on spectroscopic and chemical regeneration criteria (17).

## MATERIALS AND METHODS

The photoreceptor membranes were prepared according to the method of DeGrip et al. (18) from frozen cattle retina (Hormel Austin, Minn.) and then spun-dried into films as described in references 4 and 6. The rhodopsin in these films has been shown to maintain the same relative orientation as in the disk membrane (4). Furthermore, ultraviolet and visible absorption spectroscopy, photobleaching and regeneration by 11-*cis*-retinal in these films, all indicate that rhodopsin is structurally intact under the conditions of these experiments. Films were prepared for the purpose of infrared measurements on 0.6-mm thick AgCl windows (Wilks Scientific, South Norwalk, Conn.) or 1.5-mm thick KRS-5 windows (Harrick Scientific, Ossining, N.Y.), and for the far UVCD measurements on 0.15-mm thick quartz flats (Esco, Oak Ridge, N.J.).

All infrared (IR) spectra were recorded with a dual beam Fourier transform infrared spectrometer (Digilab FTS-14, Cambridge, Mass.) which afforded greater sensitivity and speed at low incident beam energy compared to conventional scanning instruments. Spectra were recorded at either 4 or 8  $\text{cm}^{-1}$  resolution with 50 scans of the reference and 100 scans of the sample beam, except where indicated. Measurements of linear dichroism,  $R$ , the ratio of the absorption for light polarized vertically to that horizontally, were made by mounting the sample on a single axis goniometer which could be tilted at any angle  $\alpha_0$ , about a horizontal axis arranged normal to the incident IR beam. The incident beam passed first through a wire grid polarizer (Molelectron, Sunnyvale, Calif.), the photoreceptor membrane film, and finally the AgCl or KRS-5 window which, in the case of AgCl, acted as a partial polarization scrambler. In some cases samples  $<5 \mu\text{m}$  thick were used to minimize birefringence and other artifacts. The sample was tilted at angles of 0°, 15°, 30°, 45°, and 60° and the absorption measurements recorded for horizontally polarized light (parallel to the sample tilt axis) and vertically polarized light (perpendicular to the sample tilt axis). A blank AgCl or KRS-5 window was then mounted in an identical fashion and a set of similar measurements made for all angles with horizontal and vertical polarized light. The final spectrum was determined by digitally subtracting the blank from the sample spectrum. Films were measured either in an  $\text{N}_2$ -purged IR compartment or by allowing the film to equilibrate for 1 h before measurement in a compartment containing several beakers of water. Changes in the IR spectrum which resulted from humidification were monitored; however, since not more than a 3% change in the total absorption of any one peak was found, the humidity changes over the range of our measurements did not affect the results.

Far UVCD measurements were made on a Cary model 61 spectropolarimeter (Cary Instruments, Fairfield, N.J.) at 23°C. Circular dichroic (CD) calibration was made using a standard solution of

*d*-10-camphorsulfonic acid in water (19). The dynode voltage was always <0.4 kV, the period 30 s, and the recording speed 10 nm/min. To minimize artifacts due to light scattering, linear dichroism, linear birefringence, and optical inhomogeneities we have used very thin films with absorbance at 498 nm of <0.08. In this case, we found a linear relationship between the absorbance and ellipticity for films of varying thicknesses. In addition, the light scattering of the films was not greater than that of the solution as determined by absorption spectroscopy at 650 nm. Samples for UVCD consisted either of photoreceptor membrane films equilibrated at room humidity or immersed in H<sub>2</sub>O by placing a second quartz coverslip over a sample containing a drop of H<sub>2</sub>O. All samples were unbleached during the CD measurements.

## ANALYSIS OF POLARIZED IR MEASUREMENTS

Two methods were used to determine the average alpha-helix orientation in rhodopsin. The first method is based on measuring the linear dichroism,  $R$ , of the amide I (1,657 cm<sup>-1</sup>), amide II (1,545 cm<sup>-1</sup>) and amide A (3,300 cm<sup>-1</sup>) bands as a function of the angle  $\alpha_0$  (15). Since it has been determined that these peaks reflect strongly the alpha-helix conformation in rhodopsin (9, 10), it is possible to relate the linear dichroism for each of these peaks to an effective order parameter,  $p_\alpha = \langle (3 \cos^2 \theta_\alpha - 1)/2 \rangle$ , where  $\theta_\alpha$  is the angle which each alpha-helix axis makes with the membrane normal. The relevant expression (15) is:

$$R = 1 + \sin^2 \alpha \, 3p/(1 - p), \quad (1)$$

where  $\alpha_0$  is corrected for refraction in the film by  $\sin \alpha_0 = n \sin \alpha$  and  $n$ , the film refractive index at infrared wavelengths used, is estimated at 1.7 (20). The effective order parameter of a transition dipole for absorption,  $p$ , is the product of three order parameters  $p_\alpha$ ,  $p_M$ , and  $p_T$ . The latter two are the mosaic spread order parameter  $p_M = \langle (3 \cos^2 \theta_M - 1)/2 \rangle$ , where  $\theta_M$  is the angle the membrane normal makes with the film plane, and the transition moment order parameter  $p_T = \langle (3 \cos^2 \theta_T - 1)/2 \rangle$ , where  $\theta_T$  is the angle a transition dipole makes with the alpha-helix axis, which has been measured for the amide I, II, and A vibrations (21, 22). It can be seen from the above expressions that  $p_\alpha$  can be determined from the linear dichroism  $R$  only if  $p_M$ , the mosaic spread, is known. However, an upper limit estimate of  $\langle \theta_\alpha \rangle$  can be made if it is assumed that  $p_M = 1$  (i.e., membrane orientation is perfect). In the case of our photoreceptor membrane films, measurements were only possible on relatively thin samples (<5  $\mu$ m) to avoid complications due to anisotropy in refractive index which produces IR birefringence (23). These samples, however, on the basis of visual observation appeared to contain significant mosaic spread (i.e.,  $p_M < 1$ ). This is most likely due to surface imperfections on the AgCl windows. Hence, the estimates of alpha-helix tilt from linear dichroism after making the assumption  $p_M = 1$ , are likely to seriously overestimate  $\langle \theta_\alpha \rangle$ . (For a general review of the application of infrared spectroscopy to biomembranes cf. reference 24).

The second method used to estimate the alpha-helix orientation in rhodopsin is based on measuring  $S$ , the amide II/amide I ratio for a sample in vertically polarized light as a function of  $\alpha$ . We have derived an expression (cf. Appendix) which relates  $S$  to  $p_I$  and  $p_{II}$ :

$$S = 0.45 \frac{p_{II}(3 \sin^2 \alpha - 1) + 1}{p_I(3 \sin^2 \alpha - 1) + 1}, \quad (2)$$

where  $p_I$  and  $p_{II}$  are the effective order parameters for the amide I and amide II transition

moments and are related to  $p_\alpha$  by  $p_I = p_\alpha p_M p_{T_I}$  and  $p_{II} = p_\alpha p_M p_{T_{II}}$ . The coefficient 0.45 is derived from the  $S$  value found for a random suspension of alpha-helical proteins and polypeptides (25). With this method, it is again necessary to know  $p_M$  to determine  $p_\alpha$ . However, thicker samples, which have a lower mosaic spread, can be used to obtain a more accurate estimate of  $\langle \theta_\alpha \rangle$  when  $\alpha = 0^\circ$  since birefringence should be absent at normal incidence.

## RESULTS AND DISCUSSION

### *Infrared Measurements*

Figs. 1 and 2 show the IR spectra of a photoreceptor membrane film from 1,000 to 1,800  $\text{cm}^{-1}$  and 2,800 to 3,600  $\text{cm}^{-1}$ , respectively, for the angles  $\alpha_0 = 0^\circ, 30^\circ, 45^\circ$ , and  $60^\circ$  and light

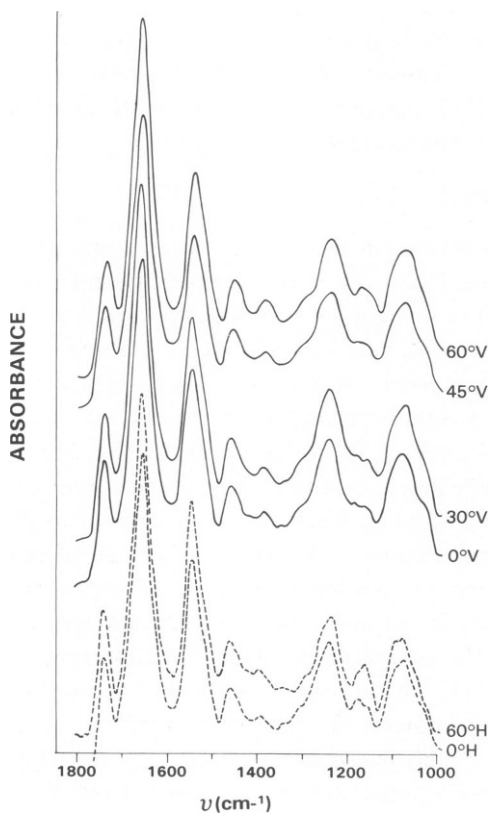


FIGURE 1

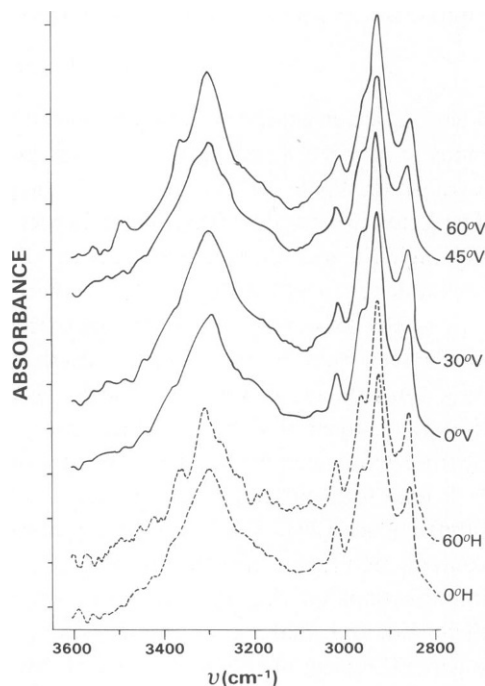


FIGURE 2

FIGURE 1 Polarized Fourier transform infrared spectra of a partially bleached cattle photoreceptor membrane film from 1,000 to 1,800  $\text{cm}^{-1}$ . The sample was prepared on AgCl window using the isopotential spin-dry method. Spectra were obtained at room temperature with 200 scans of the sample and 100 scans of the reference beam at 8  $\text{cm}^{-1}$  resolution. The tilt angle of the sample and the polarization are indicated in the spectra. The sample had an optical density at 498 nm of 0.05. The marks in the absorbance axis are separated by 0.04 o.d. for the 45° and 60° spectra, and by 0.03 o.d. for the 0° and 30° spectra.

FIGURE 2 Same as Fig. 1. Spectra from 2,800 to 3,600  $\text{cm}^{-1}$ .

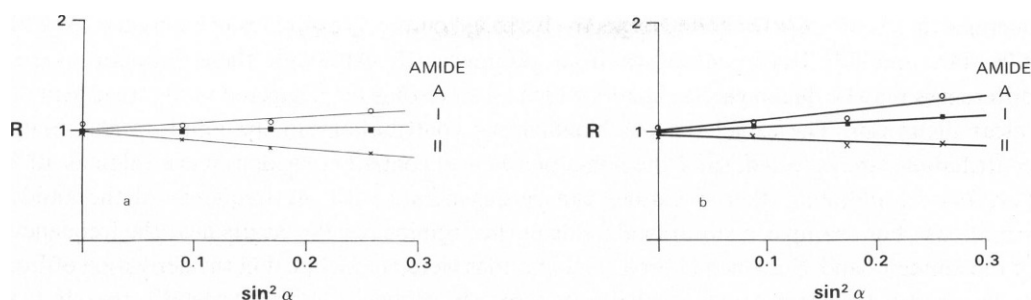


FIGURE 3 (a) Dependence of the dichroic ratio  $R$  on  $\sin^2 \alpha$  for the amide I, II, and A vibrations. The data shown in Figs. 1 and 2 were used, and the absorption intensity of the peaks was taken as the peak maximum using as base lines: a straight line from 1,800 to 1,350  $\text{cm}^{-1}$  for the amide I and II bands, and a line from 3,700  $\text{cm}^{-1}$  parallel to the  $x$  axis for the amide A band. Other base lines resulted in little change in the dichroism result. The slopes found using least-square fit were: amide A,  $0.64 \pm 0.28$ ; amide I,  $0.17 \pm 0.05$ ; amide II,  $-0.67 \pm 0.06$ . (b) Same as a with all peak absorbances normalized to the 2,925- $\text{cm}^{-1}$  peak. The slopes obtained using least-square fit were: amide A,  $1.04 \pm 0.33$ ; Amide I,  $0.51 \pm 0.07$ ; Amide II,  $-0.37 \pm 0.14$ .

polarized horizontally ( $H$ ) or vertically ( $V$ ). We find that the relative height of the peaks in the horizontal spectra remain unchanged, whereas the vertical spectra exhibit changes in relative intensity of the amide I, II, and A peaks. If we plot the dichroism,  $R = A_V/A_H$  vs.  $\sin^2 \alpha$ , straight lines are obtained (Fig. 3 a), as predicted by Eq. 1. From the slope of each of these lines we can determine  $p$ , which as discussed above gives an upper-limit estimate of  $\langle \theta_\alpha \rangle$ . The  $\langle \theta_\alpha \rangle$  calculated from the linear dichroism for the amide I, II, and A peaks is shown in Table I. Similar measurements were made on films of thicknesses ranging from 2 to 5  $\mu\text{m}$  and also for photoreceptor membrane partially bleached to Meta I as well as unbleached films. The average  $\langle \theta_\alpha \rangle$  obtained for three measurements is listed in Table I.

It is found from the linear dichroism measurements of the amide A, I, and II peaks that the

TABLE I  
ESTIMATION OF  $\langle \theta_\alpha \rangle$  FROM DICHROISM DATA

		$p_\alpha$	$\langle \theta_\alpha \rangle$
A	Amide A	0.26	45
	Amide I	0.13	50
	Amide II	0.72	26
B	Amide A	0.27	44
	Amide I	0.29	44
	Amide II	0.59	32
C	Amide A	0.39	40
	Amide I	0.36	41
	Amide II	0.35	41

The values used for the angles of the transition moments relative to the alpha-helix axis were:  $\theta_{T_A} = 28^\circ$ ,  $\theta_{T_I} = 39^\circ$ ,  $\theta_{T_{II}} = 75^\circ$  (from reference 22).

(A) Result obtained using the slopes from Fig. 3 a.

(B) Average obtained for three different films with thickness 2–5  $\mu\text{m}$ .

(C) Result obtained using the slopes from Fig. 3 b.

average  $\langle \theta_a \rangle$  is 46°, 48°, and 36°, respectively, based on the  $\theta_T$  estimates of reference 15, and 44°, 44°, and 32° based on values from reference 22. Although these estimates vary, differences may be due in part to factors which we have thus far neglected in the treatment of linear dichroism. These include: (a) Nondichroic contributions to the amide peaks. Such contributions are expected, since the non-alpha-helical content of rhodopsin is as high as 40% (11, 26). In addition, other vibrations can be degenerate with the frequency of the amide vibrations. For example, a vibrational mode of the arginine residue occurs near the frequency of the amide I band. Such nondichroic contributions were not included in the derivation of Eq. 1, hence the estimates of  $\langle \theta_a \rangle$  will be in error. It is shown in the Appendix that if the percentage of alpha-helix contribution to a particular peak in a nonoriented sample (i.e., a suspension) is  $f$ , then the experimentally obtained order parameter  $p$  is related to the real order parameter for the transition moment,  $p'$  by:

$$p = p'f. \quad (3)$$

For example, if  $f = 0.6$ , the  $p'$  of the amide A vibration is 0.30, and the  $\langle \theta_a \rangle$  is reduced from 44° to 37°. It is also expected that  $f$  will be different for each of the amide peaks, thus accounting for the differences observed in the estimated  $\langle \theta_a \rangle$ . (b) A systematic error in the absolute height of the horizontal absorption data relative to the vertical absorption as a function of  $\alpha_0$ . This could be due for example to a preferential sensitivity of the spectrometer to polarized light. We find that if all spectra are normalized against the 2,925-cm<sup>-1</sup> peak, all  $\langle \theta_a \rangle$  estimated for the amide peaks agree (Fig. 3 b and Table I). However, utilization of the 2,925-cm<sup>-1</sup> peak may not be valid, since the CH vibrations of lipids in the bilayer have been shown to be dichroic (24). (c) Optical activity and birefringence. These effects will tend to alter the light polarization as it passes through the film and can be mistaken for linear dichroism. This may be especially pronounced in liquid-crystalline film exhibiting an anisotropic index of refraction. The use of thin films should help minimize these effects. Polarized attenuated total reflection (ATR) also avoids some of these problems and yields lower  $\langle \theta_a \rangle$  values.

The second method of estimating  $\langle \theta_a \rangle$  is based on measuring the amide II/amide I ratio,  $S$ , of only the vertical absorption at different angles. Hence, error due to factor  $b$  discussed above is eliminated. An estimate of  $\langle \theta_a \rangle$  based on this method for both bleached and unbleached samples, humidified and dried, all yielded a value in the range 40°–45°. For example, Fig. 4 shows a plot of Eq. 2 for different values of  $p_a$  (assuming again  $p_M = 1$  for an upper-limit estimate of  $\langle \theta_a \rangle$ ). The values of  $S$  measured for an unbleached film in high humidity all fall near the curve corresponding to  $\langle \theta_a \rangle = 43^\circ$ . In addition, the  $S$  value at  $\alpha_0 = 0^\circ$  for thicker samples ( $>5 \mu\text{m}$ ), which appeared to have a lower mosaic spread based on relative light scattering, yielded values of  $\langle \theta_a \rangle$  in the range 37°–41° (Fig. 4). This method was also applied to data obtained from oriented purple membrane and the predicted  $\langle \theta_a \rangle$  was in close agreement with the results of linear dichroism analysis (15).

### *Circular Dichroism Measurements*

The CD spectrum for photoreceptor membrane in 1% digitonin solution is compared in Fig. 5 to photoreceptor membrane films prepared by isopotential spin-drying and also by air-drying.

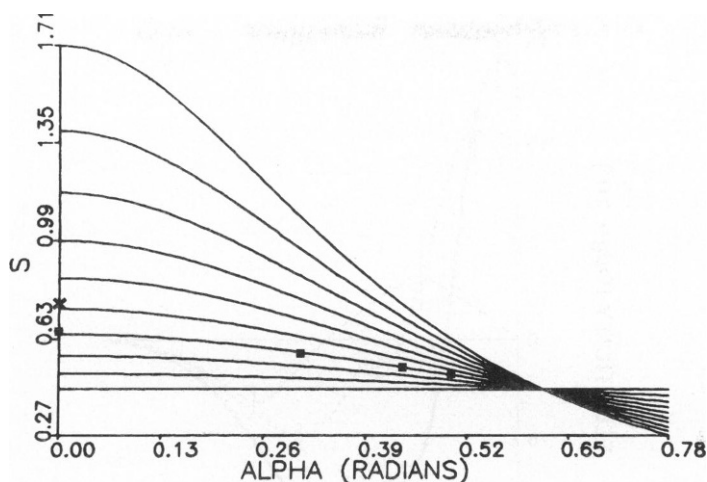


FIGURE 4 The ratio  $S$  of the amide II/amide I band intensities plotted against the sample tilt angle  $\alpha$  (related to  $\alpha_0$  through Snell's law) for values of  $p_a$  ranging from 0 (bottom curve) to 0.9 in increments of 0.1, according to Eq. 2.  $p_M$  is taken equal to 1 and the  $p_T$  values are estimated from reference 15. The squares are experimental points for an unbleached film in high humidity (absorption at 498 nm equal to 0.1 o.d.). The points fall close to the curve corresponding to  $p_a = 0.30$ , which gives  $\langle \theta_a \rangle = 43^\circ$ . The cross is an experimental value for a bleached sample in high humidity, with absorption at 498 nm equal to 0.3 o.d. For that  $S$  value (0.8) we have  $p_a = 0.45$ , which corresponds to  $\langle \theta_a \rangle = 37^\circ$ .

The spectrum of photoreceptor membrane in 1% digitonin is composed of three extrema at 221, 210, and 192 nm, with a crossover point at 203 nm in agreement with a previous study (27). In the case of air-dried films, there is a reduction in the 210-nm extremum. In addition, the band positions have red-shifted to 223, 213, and 195 nm, respectively. In the case of the isopotential spin-dried films, the 210-nm extremum has completely disappeared, the remaining peaks now appearing at  $\sim 233$  and 205 nm. The 210-nm extremum was also absent in films which were humidified or immersed in water.

The above results can be explained in terms of a model for which the rhodopsin alpha-helices are predominantly arranged normal to the membrane plane. The CD spectrum of alpha-helical polypeptides in the 190- to 250-nm spectral region normally displays extrema near 191, 208, and 222 nm (28). These bands have been studied extensively (29–35). The 222-nm band has been assigned to  $n$ - $\pi^*$  transition of the amide group (29). The 191- and 208-nm extrema are predominantly due to Moffitt bands (30, 31). These bands are allowed only for the light incident perpendicular to the alpha-helix axis (32, 33). In addition, there may be a contribution from the so-called helical bands, one positive at 199 nm and one negative at 181 nm (34, 35). The helical bands are allowed only for light propagating parallel to the helix axis (32, 33).

Hence, we expect, based on the above studies, that alpha-helices arranged parallel to the incident beam will not display the Moffitt bands, but will display activity near 199 and 222 nm. In fact, we do observe such an effect only for well-oriented photoreceptor membrane samples, in agreement with similar measurements made on oriented purple membrane (16).

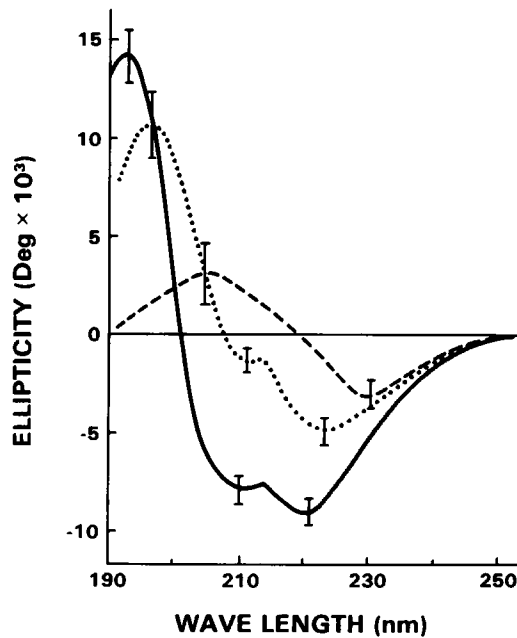


FIGURE 5 Circular dichroism of photoreceptor membrane. The far UVCD spectrum of (—) 1% digitonin solution of rhodopsin, (.....) air-dried film and (----) isopotential spin-dried film. The air-dried film was prepared by placing several drops of photoreceptor membrane solution (absorption at 498 nm < 0.08, pH 7.0) on a quartz flat and letting it dry slowly at room temperature under a dim red light. The humidity of (—) and (···) film was determined by the room conditions.

## CONCLUSIONS

From the above considerations, we conclude that rhodopsin contains a core of alpha-helices which are likely to have an effective tilt of  $<40^\circ$  from the membrane normal. This conclusion is supported by several other lines of evidence including the existence of diamagnetism in rod outer segments (36), the elongated shape of rhodopsin (37) and chemical proteolysis (11). Recent polarized IR measurements on magnetically oriented rod outer segments (ROS) also confirm this conclusion (38).

It is unknown at present whether perpendicular alpha-helices are a common feature of all integral membrane proteins, particularly those which span the bilayer, or are a special feature of rhodopsin and bacteriorhodopsin. Polarized IR on other oriented biological membranes and reconstituted membrane systems (e.g.,  $\text{Ca}^{++}$ -ATPase) should be able to provide an answer. It is also unknown whether a transverse arrangement of alpha-helices plays a structural or functional role in rhodopsin. It is possible that alpha-helices act as an essential transport bridge across the bilayer. On the other hand, the hydrophilic nature of breaks in alpha-helical regions may force most membrane protein alpha-helices to terminate at the hydrophilic surfaces of a bilayer.

## APPENDIX

### Derivation of Eqs. 2 and 3

#### EQ. 2

Consider a film rotated an angle  $\alpha_0$  about the y axis (where  $\alpha_0$  is related to  $\alpha$  through Snell's law) and irradiated with vertically polarized light. The absorption intensity can then be written:

$$A_\nu = \langle (M \cdot E_\nu)^2 \rangle = \langle (ME \sin \alpha \cos \theta + ME \cos \alpha \sin \theta \cos \phi)^2 \rangle, \quad (A1)$$

where  $M$  is the transition moment (Fig. A1). (Note, we drop the  $\nu$  subscript from  $E$ .) Since the orientational distribution of  $M$  is assumed to be independent of  $\phi$  we have:

$$A_\nu = M^2 E^2 \int \int (\sin \alpha \cos \theta + \cos \alpha \sin \theta \cos \phi)^2 f(\theta) \sin \theta d\theta d\phi. \quad (A2)$$

Simplifying Eq. A2, substituting  $x = \cos \theta$  and integrating over  $\phi$ :

$$A_\nu = M^2 E^2 \pi \left[ \int_{-1}^1 (3x^2 - 1) \sin^2 \alpha f(x) dx + \int_{-1}^1 (1 - x^2) f(x) dx \right] \quad (A3)$$

Using the definition of the Legendre polynomials:  $P_2(x) = (3x^2 - 1)/2$  and  $P_0(x) = 1$ , we can write Eq. A3 as:

$$A_\nu = 2/3 M^2 E^2 \pi [p(3 \sin^2 \alpha - 1) + 1], \quad (A4)$$

with  $p = \langle P_2 \rangle$ . The ratio  $S$  of the absorption intensity for the amide I and II transition moments is then:

$$S = \frac{M_{II}^2}{M_I^2} \frac{p_{II}(3 \sin^2 \alpha - 1) + 1}{p_I(3 \sin^2 \alpha - 1) + 1}. \quad (A5)$$

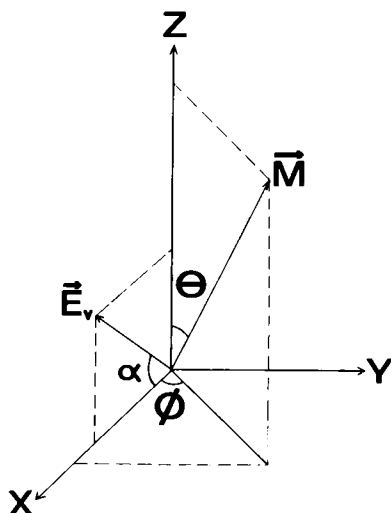


FIGURE A1 Coordinate system of film ( $x$ - $y$  plane). Transition moment of vibration,  $M$ , makes an angle,  $\theta$ , with the  $z$  axis. Vertical electric vector,  $E_v$ , makes an angle,  $\alpha$ , with the  $x$  axis. In the laboratory frame the rotation of the film is about the  $y$  axis.

### EQ. 3

For a protein which is 100%  $\alpha$ -helical, we have for the dichroic ratio:

$$R = \frac{A_V}{A_H} = 1 + \sin^2 \alpha \, 3p/(1 - p). \quad (\text{A6})$$

If only a fraction  $f'$  of the peak at  $\alpha_0 = 0^\circ$  is due to  $\alpha$ -helices, we can define the quantity  $R'$ , the dichroic ratio which would be observed if all non-alpha-helical contributions were absent.  $R'$  is related to the absorbance due to alpha-helix contributions,  $A_\alpha$ , by:

$$R' = \frac{(A_\alpha)_V}{(A_\alpha)_H} = 1 + \sin^2 \alpha \, 3p'/(1 - p'), \quad (\text{A7})$$

where  $p'$  is the theoretical order parameter which would be found if one could measure the linear dichroism of the  $\alpha$ -helices unaffected by non-alpha-helical contributions. We also have the relations:

$$A_H = (A_\alpha)_H + A_{n\alpha}, \quad A_V = (A_\alpha)_V + A_{n\alpha}, \quad (\text{A8})$$

where  $A_{n\alpha}$  is the non-alpha-helical part of the total absorbance, assumed to be non-dichroic. We can now relate  $R$  and  $R'$  as follows:

$$R - 1 = \frac{A_V}{A_H} - 1 = \frac{(A_\alpha)_V - (A_\alpha)_H}{A_H} = \frac{(A_\alpha)_H}{A_H} \left( \frac{(A_\alpha)_V}{(A_\alpha)_H} - 1 \right), \quad (\text{A9})$$

which reduces upon simplification to:

$$R - 1 = f' (R' - 1), \quad (\text{A10})$$

where  $f' = (A_\alpha)_H/A_H$ . Hence, using Eqs. A7 and A10:

$$f' 3p'/(1 - p') = 3p/(1 - p). \quad (\text{A11})$$

We now relate  $f'$  to  $f$ , the percentage of the absorption of a particular peak due to alpha-helices in a nonoriented (i.e., random) sample. If the total absorption is  $T$ , then the alpha-helix contribution by definition is  $fT$  and the non-alpha-helical contribution  $T(1 - f)$ . If we now orient the sample, the absorption for the alpha-helical dichroic contribution will be  $Tf(1 - p')$ , where  $p'$  is the order parameter. The nondichroic contribution will remain unchanged. Hence, the total fraction of the alpha-helix absorption in the oriented sample will be:

$$f' = f(1 - p')/(1 - fp'), \quad (\text{A12})$$

and inserting this into Eq. A11 we have the relation:

$$3p/(1 - p) = 3p'f/(1 - p'f). \quad (\text{A13})$$

Thus we may write:

$$p = fp'. \quad (\text{A14})$$

We wish to thank W. DeGrip, J. Korenbrot, and P. Brown for helpful discussions, and V. Culbertson and K. M. Rosen for technical assistance.

This work was supported by an American Heart Association Established Investigatorship and a grant from the National Institutes of Health-National Eye Institute to K. J. Rothschild, and Fundação de Amparo à Pesquisa do Estado de São Paulo, Brazil (R. Sanches). Polarized infrared spectroscopy was done at the Material Science Center at Massachusetts Institute of Technology, Cambridge, Mass.

*Received for publication 31 October 1979 and in revised form 26 February 1980.*

## REFERENCES

1. SINGER, S. J., and G. L. NICOLSON. 1972. The fluid mosaic model of the structure of cell membranes. *Science (Wash. D. C.)* **175**:720.
2. LEVINE, Y. K., A. T. BAILEY, and M. H. F. WILKINS. 1968. Multilayers of phospholipid bimolecular leaflets. *Nature (Lond.)* **22**:577.
3. HERBETTE, L., J. MARQUARDT, A. SCARPA, and J. K. BLASIE. 1977. A direct analysis of lamellar x-ray diffraction from hydrated multilayers of fully functional sarcoplasmic reticulum. *Biophys. J.* **20**:245.
4. ROTHSCILD, K. J., N. A. CLARK, and K. M. ROSEN. 1980. Incorporation of photoreceptor membrane into a multilamellar film. *Biophys. J.* **31**:45-52.
5. ROTHSCILD, K. J., N. A. CLARK, K. M. ROSEN, R. SANCHES, and T. L. HSIAO. 1980. Spectroscopic study of photoreceptor membrane incorporated into a multilamellar film. *Biochem. Biophys. Res. Commun.* **92**:1266.
6. CLARK, N. A., K. J. ROTHSCILD, B. A. SIMON, and D. A. LUIPPOLD. 1980. Surface induced orientation of multilayer membrane arrays: theoretical analysis and a new method with application to purple membrane fragments. *Biophys. J.* **31**:65-96.
7. EBREY, T. G., and B. HONIG. 1975. Molecular aspects of photoreceptor function. *Quart. Rev. Biophys.* **8**:129.
8. ROTHSCILD, K. J., J. R. ANDREW, W. J. DEGRIP, and H. E. STANLEY. 1976. Opsin structure probed by Raman spectroscopy of photoreceptor membranes. *Science (Wash. D. C.)* **191**:1176.
9. OSBORNE, H. B. and E. NABEDRYK-VIALA. 1977. The hydrophobic heart of rhodopsin revealed by an infrared  $^1\text{H}$ - $^2\text{H}$  exchange study. *FEBS Lett.* **84**:217.
10. ROTHSCILD, K. J., W. J. DEGRIP, and R. SANCHES. 1980. Fourier transform infrared study of photoreceptor membrane. I. Group assignments based on rhodopsin delipidation and reconstitution. *Biochim. Biophys. Acta.* **596**:338.
11. LITMAN, B. J. 1979. Rhodopsin: its molecular substructure and phospholipid interactions. *Photochem. Photobiol.* **29**:671.
12. ADAMS, A. J., R. L. SOMERS, and H. SHICHI. 1979. Spatial arrangement of rhodopsin in the disk membrane as studied by enzymatic labeling. *Photochem. Photobiol.* **29**:687.
13. STOECKENIUS, W., R. H. LOZIER, and R. A. BOGOMOLNI. 1979. Bacteriorhodopsin and the purple membrane of Halobacteria. *Biochim. Biophys. Acta.* **505**:215.
14. HENDERSON, R., and P. N. T. UNWIN. 1975. Three-dimensional model of purple membrane obtained by electron microscopy. *Nature (Lond.)* **275**:28.
15. ROTHSCILD, K. J., and N. A. CLARK. 1979. Polarized infrared spectroscopy of oriented purple membrane. *Biophys. J.* **25**:473.
16. MUCCIO, D. D., and J. Y. CASSIM. 1979. Interpretation of the absorption and circular dichroic spectra of oriented purple membrane films. *Biophys. J.* **26**:427.
17. BRIDGES, C. D. B. 1970. In *Biochemistry of the Eye*. (C. N. Graymore, editor.) Ch. 9. Academic Press, Inc., New York.
18. DEGRIP, W. J., F. J. M. DAEMEN, and S. L. BONTING. 1979. *Methods Enzymol.* In press.
19. CASSIM, J. Y., and J. T. YANG. 1969. A computerized calibration of the circular dichrometer. *Biochemistry.* **8**:1947.
20. HENNIKER, C. J. 1973. Infrared refractive indices of some oriented polymers. *Macromol. Rev.* **6**:514.
21. AMBROSE, E. J., and A. ELLIOT. 1951. The structure of synthetic polypeptides. II. Investigation with polarized infrared spectroscopy. *Proc. Roy. Soc. Lond. A. Math. Phys. Sci.* **205**:47.
22. TSUBOI, M. 1962. Infrared dichroism and molecular conformation of alpha-form poly- $\gamma$ -benzyl-L-glutamate. *J. Polym. Sci. Part D Macromol. Rev.* **59**:139.
23. SUSI, H. 1969. In *Structure and Stability of Biological Macromolecules*. S. N. Timasheff and G. D. Fasman, editors. Marcel Dekker, New York. 575.
24. WALLACH, D. F. H., P. V. SURENDRA, and J. FOOKSON. 1979. Application of laser Raman and infrared spectroscopy to the analysis of membrane structure. *Biochim. Biophys. Acta.* **559**:153.
25. BLOUT, E. R., C. DE LOZE, and A. J. ASADOURIAN. 1961. The deuterium exchange of water-soluble polypeptides and proteins as measured by infrared spectroscopy. *J. Am. Chem. Soc.* **83**:1895.
26. STUBBS, G. W., H. G. SMITH, and B. J. LITMAN. 1976. Alkyl glucosides as effective solubilizing agents for bovine rhodopsin: a comparison with several commonly used detergents. *Biochim. Biophys. Acta.* **426**:46.
27. RAFFERTY, C. N., J. Y. CASSIM, and D. G. MCCONNELL. 1977. Circular dichroism, optical rotatory dispersion, and absorption studies on the conformation of bovine rhodopsin in situ and solubilized with detergent. *Biophys. Struct. Mech.* **2**:277.
28. HOLZWARTH, G., and P. DOTY. 1965. The ultraviolet circular dichroism of polypeptides. *J. Am. Chem. Soc.* **81**:218.

29. WOODY, R. W. 1968. Improved calculations of the  $n$ - $\pi^*$  rotational strength in polypeptides. *J. Chem. Phys.* **49**:4797.
30. MOFFITT, W. 1956. Optical rotatory dispersion of helical polymers. *J. Chem. Phys.* **25**:467.
31. TINOCO, I., JR. 1964. Circular dichroism and rotatory dispersion curves for helices. *J. Am. Chem. Soc.* **86**:297.
32. MANDEL, R., and G. HOLZWARTH. 1972. Circular dichroism of oriented helical polypeptides: the alpha-helix. *J. Chem. Phys.* **57**:3469.
33. SNIR, J., and J. SCHELLMAN. 1973. Optical activity of oriented helices. Quadrupole contributions. *J. Phys. Chem.* **77**:1653.
34. WOODY, R. W., and I. TINOCO, JR. 1967. Optical rotation of oriented helices. III. Calculations of the rotatory dispersion and circular dichroism of the alpha- and  $3_{10}$ -helix. *J. Chem. Phys.* **46**:4927.
35. LOXSOM, F. M. 1969. Optical rotation of helical polymers: periodic boundary conditions. *J. Chem. Phys.* **51**:4899.
36. CHABRE, M. 1978. Diamagnetic anisotropy and orientation of  $\alpha$ -helix in frog rhodopsin and meta II intermediate. *Proc. Natl. Acad. Sci. U.S.A.* **75**:5471.
37. WU, C. W., and L. STRYER. 1972. Proximity relationships in rhodopsin. *Proc. Natl. Acad. Sci. U.S.A.* **69**:1104.
38. M. MICHEL-VILLAZ, SAIBIL, H., and M. CHABRE. 1979. Orientation of alpha-helical segments in retinal rod outer segments studied by infra-red linear dichroism. *Proc. Natl. Acad. Sci. U.S.A.* **76**:4405.